

A New Method for Tolerance Integration in CAD Model

Mehdi Tlija^{#1}, Borhen Louhichi^{#1,2}, Abdelmajid BenAmara^{#1}

^{#1} LGM, ENIM, University of Monastir, Av. Ibn Eljazzar 5019 Monastir, Tunisia
tlija.mehdi@gmail.com

^{#2} LIPPS, ÉTS, 1100, Notre-Dame Ouest, Montréal, H3C1K3, Québec, Canada
Borhen.Louhichi@etsmtl.ca

Abstract— In the Digital Mock-Up (DMU), the parts and the assemblies are used in the nominal configurations. In fact, the tolerances are formally represented in CAD model and the impacts of tolerance stack-up are not considered during the optimization of the mechanical system assemblability and the F.E. Analysis. Then, the improvement of the numerical model requires the tolerance consideration in the CAD model.

This paper presents an approach to incorporate dimensional and geometrical tolerances in CAD model. The models to obtain worst case components are developed. The worst case assemblies can be obtained by performing various combinations between the components in worst case configurations. Nevertheless, the regeneration of the worst case assemblies, composed by the realistic components, requires redefining assembly mating constraints which are initially allocated to the nominal assembly. Thus, in the case of rigid body, a new approach to update the mating constraints of a realistic assembly is presented.

Keywords— CAD model, mating constraint, dimensional tolerance, geometrical tolerance, realistic model.

I. INTRODUCTION

The virtual model is used to improve mechanical design process. In the concurrent engineering, design process is supported by many tools and phases (analysis, manufacturing, tolerancing...). The tolerancing is a technical tool for obtaining a good compromise between quality and price. In CAD model, the tolerance integration is performed by obtaining the parts and the assemblies in the configurations with defects: these configurations represent the realistic models. This modelling means to envisage the tolerance impact on the assemblability and functioning of the mechanical systems.

Several researches had contributed to developing methodologies of tolerance analysis and syntheses for a good choice of specifications. The CLIC (Tolerancing in Localization with Influence of the Contacts) method allows choosing the adequate dimensional and geometric specifications for a mechanism [1]. CLIC is CAT (Computer aided tolerancing) software based on three-dimensional computation. In addition, static and three dimensional tolerancing models are developed to optimize tolerance values of functional requirements [2], [3].

The prediction of geometrical deviations between the real and the ideal assembly and the optimization of the resulting stress had been intensively investigated by researches. Socoliuc et al. established an approach to realize a realistic simulation of assemblies [4]. This approach is based on TTRS (Topologically and technologically related surfaces) model [5].

Indeed, a complex mechanical system is represented by a simple parametric model. Then, the point deviations, which are located on the toleranced face, are modelled by the polyhedral tool [6]. Therefore, the tolerance effects on functional requirements of the assembly are obtained. Nevertheless, the polyhedral is a difficult tool to be used on the industry. This model does not predict the impact of dimensional and geometrical deviations, permitted by tolerances, on the assembly deformations. Pierre et al. developed a method to take into account both the thermo-mechanical effects and the geometrical defects of assembly by using the three dimensional chain tools [7]. The model is based on the substitute surface approach. The method presents a solution, in torsorial form, for the problems of coupling between the thermal requests and the geometrical defects. This tool was improved by proposing a vectorial method for tolerance analysis. The model improvement was also performed by using the common surfaces in contact between the assembled parts [8]. The solutions are presented in mathematical form (equations) and not modelled in a geometric solution. Mandil et al. proposed a conceptual study of a functional requirement computation given at several stages of the product life cycle management [9].

In this paper, we propose a CAD model taking into account the dimensional and geometrical tolerances by giving realistic configurations of the assembly. This model is based on the assumption that the worst assembly is obtained by the components on worst case configurations. The principle of independence (ISO 8015) is respected. Indeed, in the proposed model, each tolerance is treated separately. Thereafter, two algorithms were developed in our previous works [10]-[12]: The first one leads to obtain component with dimensional defects. The second one is interested in the geometrical tolerances. In this document, the two algorithms to take account dimensional and geometrical tolerances are described shortly. Then, a method to update mating constraints of realistic assemblies is shown.

II. WORST CASE CONFIGURATIONS OF THE COMPONENT

A. Component with dimensional defects

A model was developed to obtain the worst case configurations of the component according to dimensional tolerances: Maximum and Least Material Configurations (MMC and LMC). In the general case, the designer defines the component model by using driving dimensions. In the following step, he assigns the tolerances at the driven

dimensions. The determination of the realistic components requires the identification of the relationships between the dimensions and the determination of the tolerance value to allocate on the driving dimensions. Indeed, it is necessary to detect the n driving dimensions D_i , with VD_i values, that control the driven dimension R_j (with VR_j value). The influence coefficient ij is the ratio between the variation of the driving dimension VD_i and the variation of the driven dimension VR_j (Eq.1).

$$ij = \frac{VD_i}{VR_j} \quad (1)$$

ij can be determined by using two methods: numerical perturbation method and the Dimension Vectorization Method (DVM) [11] (Fig. 1).

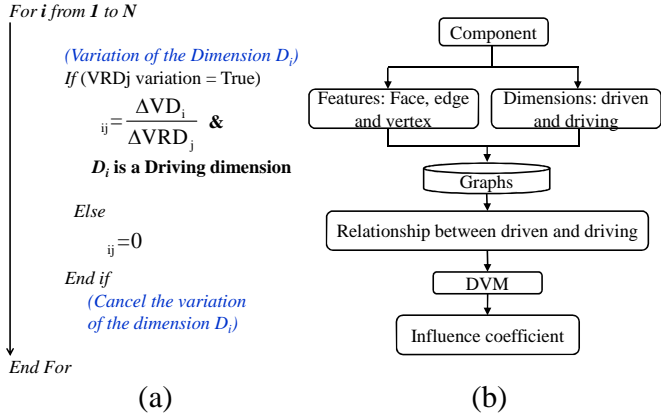


Fig. 1 Sub- algorithm for determination ij (a) by numerical perturbation. (b) by DVM.

The numerical perturbation method is based on the determination of the impact of a numerical change of the dimension value on CAD model. From numerical viewpoint, this change can be defined as a percentage ($VD_i = 0.1\% \cdot VD_i$). Initially, a perturbation value is added to each VD_i . Then, new driving dimension values $V'D_i$ ($V'D_i = VD_i + VD_i$) are obtained. For each change of driving dimension value, if the driven dimension value VR_j changes to a value VR'_j , then the two dimensions (D_i and R'_j) are in relationship. VR_{Di} is the deviation between VR'_j and VR_j ($VR_{Di} = VR'_j - VR_j$) and ij is determined by using the equation (Eq.1). The method depends on CAD model and the number of the iterations increases with the number of dimensions defined in the model.

By using the DVM, the automatic identification of relationships between all component dimensions is realised by using a technique based on connected graphs. Indeed, these graphs allow the generating three-dimensional dimension chains and the aggregation of component information. Then, the quantification of the influence between the dimensions is achieved by the vectorial modelling of the dimensions. This method consists in representing dimensions by vectors. Then, the projection of these vectors on the coordinate system of the part allows determining the influence coefficient (ij) between the dimensions.

In MMC and LMC, the extreme values of the driven dimension are obtained by uniform distribution of the tolerances to driving dimension values. The relation between

terminals of tolerance interval $[T_i^{lower}, T_i^{higher}]$ of D_i and the corresponding terminals of tolerance interval $[t_j^{lower}, t_j^{higher}]$ of R_j is given by the relation in (Eq. 2).

$$\begin{cases} \text{If } \lambda_{ij} > 0 \text{ Then } \begin{cases} T_i^{higher} = \lambda_{ij} \times t_j^{higher} / n \\ T_i^{lower} = \lambda_{ij} \times t_j^{lower} / n \end{cases} \\ \text{If } \lambda_{ij} < 0 \text{ Then } \begin{cases} T_i^{lower} = \lambda_{ij} \times t_j^{higher} / n \\ T_i^{higher} = \lambda_{ij} \times t_j^{lower} / n \end{cases} \end{cases} \quad (2)$$

Then, the method to obtain D_i values in MMC and LMC is shown in Eq.3.

$$\begin{array}{ll} \text{In MMC:} & \text{In LMC:} \\ \text{If } \lambda_{ij} > 0 \text{ then } D_i = D_i + T_i^{higher} & \text{If } \lambda_{ij} > 0 \text{ then } D_i = D_i + T_i^{lower} \\ \text{If } \lambda_{ij} < 0 \text{ then } D_i = D_i + T_i^{lower} & \text{If } \lambda_{ij} < 0 \text{ then } D_i = D_i + T_i^{higher} \end{array} \quad (3)$$

B. Component with geometrical defects

Respecting the geometrical tolerances, the worst case configurations of the component are obtained by the displacements of the toleranced features. The displacement parameters are defined by using the domain method and the worst case approach [6]. The deviation between the nominal and the realistic feature is determined by the SDT (Small Displacement Torsor) tool. Then, the form deviations are neglected relative to those of orientation and position. The method to determine worst case configurations depends on the the toleranced feature geometry and the tolerance type. The realization of the face displacements and the identification of the toleranced features the tolerance types are automated. The model was applied to the several cases: cylindrical tolerance zone, planar face with quadratic loop and planar face with complex loop. In the last case, the oriented bounding box tool was developed [11].

C. A simple example

In the Fig. 2, only some functional requirements of the piston component are illustrated to simplify the illustration.

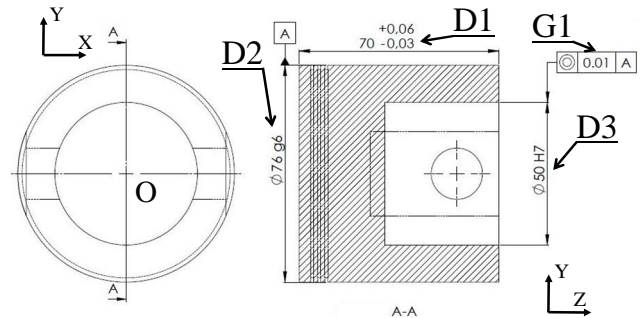


Fig. 2 Functional requirements of the piston.

The graphs method shows that the driven dimension ($D1$) is controlled by the driving dimensions ($D11$, $D12$ and $D13$) (Fig. 3 (a)). Also, $D2$ and $D3$ are influenced by $D21$ and $D31$ respectively. Then, the influence coefficients are determined by DVM. From where, the two desired configurations are obtained: MMC and LMC (Fig. 3 (b)).

The worst case configurations is obtained by applying the domains method to the coaxiality constraint (G1) (case of cylindrical tolerance zone). Then, a discretization of this tolerance zone is necessary [13]. This discretization can be performed by an angle $\alpha_k = 2k/n$; $k=1$ to n ; where n is the parameter of the discretization smoothness [13]. The parameter n is chosen by the user according to the desired numbers of configurations and the accuracy of the results.

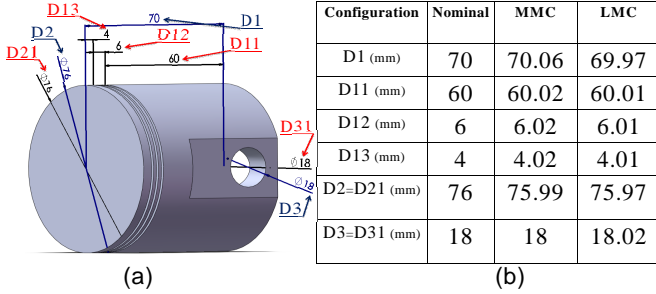


Fig. 3 (a) Nominal Configuration, (b) Dimension values in the three configurations.

For the circular loop, the face normal vectors at the edge ends are defined in the coordinate system $(O, \bar{X}, \bar{Y}, \bar{Z})$ (O is the middle point of the nominal axis) by the following vector: $\vec{n}_k = (\cos(\alpha), \sin(\alpha), 0)$.

For the studied example, we propose a discretization by an angle $\alpha_k = k/6$. Thus, 12 extreme positions of the axis are deduced. The tolerances are modelled on CAD model by movement of tolerated element (cylinder axis). The displacement parameters (rotation or translation) are deduced from the discretization. In the figure (Fig. 4), all the displacements are amplified for easier viewing. The figure (Fig. 4) shows two case of translation of the tolerated face: The first is along the axis \vec{n}_3 (Fig. 4. (a)) and the second is along the axis \vec{n}_9 (Fig. 4. (b)). The figure (Fig. 4. (c) and (d)) represent the rotation of the face by an angle $(\arctg(0.01/70))$ radians about the axis \vec{n}_9 and the axis \vec{n}_3 respectively.

III. WORST CASE CONFIGURATIONS OF THE ASSEMBLY

The relative positions of components are defined in CAD software by the mating constraints [14]. In fact, these constraints must define kinematic joints between the parts and satisfy the functional requirements for the proper functioning of the system. The component positioning can be done sequentially or simultaneously. The technique of mounting components simultaneously is insufficient in some cases [15]. Indeed, the solution, founded by using this technique, can be not optimal as the assembly of four bars of a picture frame. In CAD software, a primitive relations or high-level primitive relations are used for specifying assembly information. Then, the aggregation of assembly information in assembly models can be made by relational or hierarchical models. In this paper, sequential assembly technique is adopted in the proposed study.

In the Digital Muck-Up (DMU), the allocation of assembly mates leads to three types of assembly: under-constrained, fully constrained and over-constrained. The first, the under-constrained assembly is a system that has at least one DoF. The second type of assembly does not have any relative movement between the components. The last type of assembly is obtained when the assembly mates are conflicting and cannot be satisfied. Indeed, the geometric modeller cannot found a solution for positioning the components with required mates.

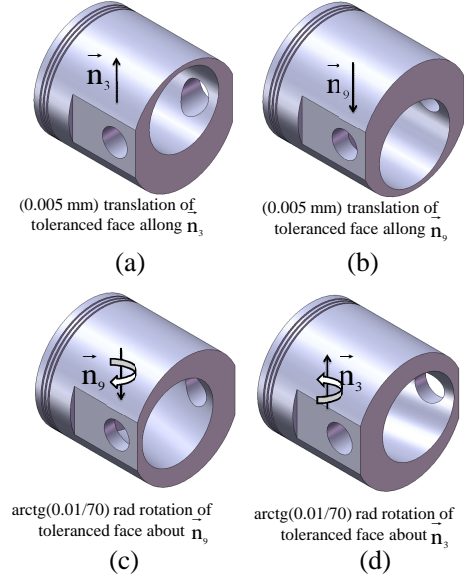


Fig. 4 (a), (b), (c) and (d) realistic models.

In this paper, a method to update the mating constraints of fully or under constrained rigid assemblies is presented. The primitive mating constraints considered are the coincident between planar faces and the coaxiality. In the realistic assembly, mate updating is realized by defining realistic primitive joints. These realistic joints are obtained by using coincidence mates between MGREs (Minimum Geometrical Reference Elements) [5]. The method depends on the Objective Functions of the Assembly (OFA) specified by the designer. In CAD software, the OFA are deduced from the nominal model: The mating constraint order, specified in the feature manager design tree of the software, defines the mounting order of the assembly and the joint order priority. The kinematic status of the nominal assembly defines the DOFs witch to be conserved in the realistic model. The DoF is identified by a method based on the graphs of primitive kinematic joints: Each assembly or sub-assembly is defined with a graph. In a graph, a node represent a part, an edge represents a primitive joint.

A. Fully constrained assembly

A fully constrained assembly of two nominal parts I and 2 (Fig. 5(a)) can be obtained by using three coincident constraints between planar faces. In the proposed realistic model, the primitive coincident constraint between two planes, which is specified in nominal model, can be modelled by the coincident constraint between: plane and plane (Co: $P\&P$),

plane and edge (Co: $P\&E$) or plane and vertex (Co: $P\&V$). The OFA composed by the two nominal parts 1 and 2 (Fig. 5 (a)) are deduced from the nominal assembly model:

- The mounting of nominal parts 1 and 2 is to be performed sequentially in the following order: $L1$ (Co: $F1.1\&F2.1$), $L2$ (Co: $F1.2\&F2.2$) and $L3$ (Co: $F1.3\&F2.3$).
- The planar faces $F1.1$ and $F2.1$ are in contact.
- The assembly is fully constrained (No DoF of assembly is allowed).

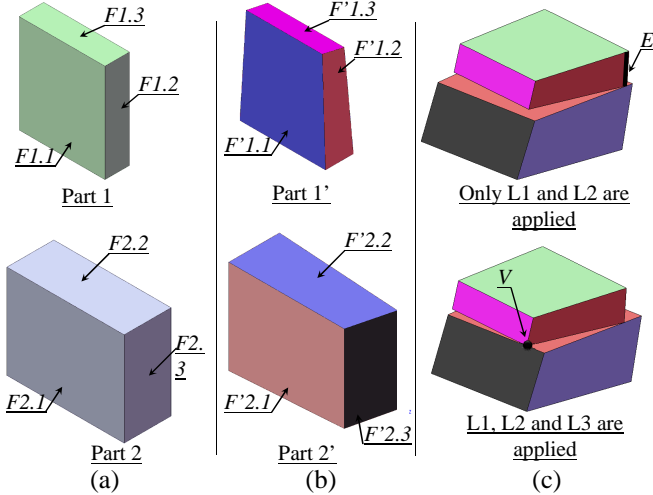


Fig. 5 (a) Nominal parts 1 and 2. (b) Realistic parts 1' and 2'. (c) Realistic assemblies.

In Fig. 5(b), the parts 1' and 2' are one of the possible realistic configurations deduced respectively from the parts 1 and 2 (sizes of face displacements are amplified for better illustration). The assembly of these two realistic parts by using the $L1$, $L2$ and $L3$ constraints is impossible and gives an over-constrained solution. The developed algorithm to update the assembly mating comprises two main steps: Verification of the relative position of the two planar faces and the choice of the mating assembly type. The method depends on the nominal relative position of the two planar faces: Contact (as $F1.1$ and $F2.1$) or without contact (as $F1.2$ and $F2.2$).

1) The case of two planar faces initially in contact

The sub-algorithm VRPTFC (to Verify Relative Position of Two Faces initially in Contact) ensures that the relative position of the two faces $F1$ and $F2$ of the parts $A1$ and $A2$ respectively is adequate (Fig. 6 (a)). $N1$ and $N2$ are the two normal vectors of $F1$ and $F2$ respectively. The vertices P_i ($i=1$ to 4) and J_j ($j=1$ to 4) are the four vertices that delimit $F1$ and $F2$ respectively. P is the plane derived from $F2$. In the realistic configuration, both faces can have three main configurations (Fig. 6 (b)):

- In the first case, the following condition is satisfied: $\overline{N1.N2} \leq 0$ and $\overline{PiJj.N1} > 0$ for $i, j = 1$ to 4. The two faces are in the correct configuration and the both faces do not intersect.

- In the second case, the condition ($\overline{N1.N2} > 0$) is satisfied. The part $A1$ is rotated about the (O, \overline{T}) axis by an angle equal to α . O is the center of the $F1$ and \overline{T} is the tangential axis to $F1$. After the part rotation, the configuration of the two faces $F1$ and $F2$ becomes similar to the configuration in first case.

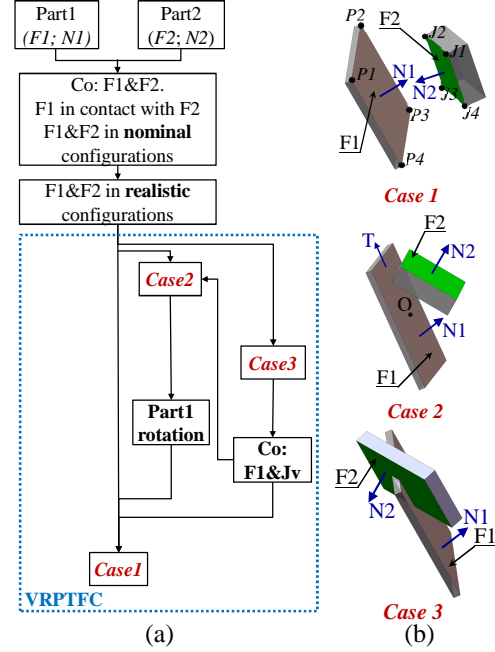


Fig. 6. (a) The sub-algorithm VRPTFC. (b) Three initial cases identified by the sub-algorithm VRPTFC.

- In the third case, the condition ($\overline{N1.N2} \leq 0$ and for $i, j = 1$ to 4 and there exists a pair (k, m) such that $\overline{PkJm.N1} < 0$) is satisfied. A coincidence constraint between the $F1$ and the vertex Jv is applied temporarily (Applied then deleted from the model). The vertex Jv is determined by the relation (Eq. 4). Then, the model becomes one of the two previous configurations (case1 or case2).

$$\begin{cases} d_{km} = \|\overline{PkJm.N1}\|; \text{ such as } \overline{PkJm.N1} < 0. \\ d_v = \|\overline{PkJv.N1}\|; \text{ such as } d_v = \max(d_{km}); k, m=1 \text{ to } 4. \end{cases} \quad (4)$$

Then, the mating constraints are conserved (Co: $P\&P$) or replaced by the assembly constraints which allow more DoF ((Co: $P\&V$) or (Co: $P\&E$)) according to the OFA:

- *Case of Co: $F\&V$:* To apply a coincident constraint between $F1$ and a vertex Sa of $F2$, a vertex Sa is to be identified. P is the plane derived from $F2$. Initially, $F2$ is discretized. The discretization method depends on the type of the face loop. In the case of quadratic loop the discretization is performed by two parameters n and m (Fig. 7). The face with circular contour is discretized by two polar parameters r and θ . For the face with complex loop, the discretization

is performed by a fine tessellation. These discretization parameters are chosen by the designer according to the desired accuracy of the results. The explication will be limited to the case of face with quadratic loop. $F1$ is modelled by a grid of vertices P_{nm} . Then, all vertices P_{nm} are projected on the plane P according $N1$ to obtain the set of vertices J_{nm} . Finally, the distance d_{min} is the minimum distance between pairs (P_{nm}, J_{nm}) and the vertex Sa is identified by the relation (Eq. 5).

$$\begin{cases} d_{min} = \min \| \overline{J_{nm} P_{nm}} \|; \text{ such as } J_{nm} \in F2 \\ Sa = J_{nm}; \text{ such as } \| \overline{J_{nm} P_{nm}} \| = d_{min} \end{cases} \quad (5)$$

- *Case of Co:F&E*: To determine the edge E it suffices to identify the two vertices $V1$ and $V2$ ($E = [V1V2]$). The face $F2$ is discretized by using the method described previously. The first vertex $V1$ is determined by the relation (Eq. 5). The second vertex $V2$ is identified by the equation (Eq. 6).

$$\begin{cases} d'_{min} = \min \| \overline{J_{nm} P_{nm}} \|; \text{ such as } J_{nm} \in F2 \text{ and } J_{nm} \neq Sa \\ V2 = J_{nm}; \text{ such as } \| \overline{J_{nm} P_{nm}} \| = d'_{min} \end{cases} \quad (6)$$

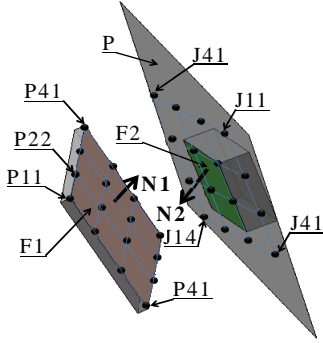


Fig. 7. Determination of the tangent vertex between two faces by the surface modelling by a grid.

2) The case of two planar face without contact in the nominal configuration

In the nominal assembly, a coincident constraint between two faces $F1$ and $F2$ of two parts $A1$ and $A2$ is applied such as the two faces are not in contact. In the realistic assembly, the relative position of $F1$ and $F2$ is verified by using a sub-algorithm to Verify Relative Position of Two Faces initially Without Contact (VRPTFWC) (Fig. 8). $N1$ and $N2$ are the two normal vectors of $F1$ and $F2$ respectively. In nominal configuration, both faces can have two main initial configurations NCase1 and NCase2 defined by the relation (Eq. 7). The relative position of the two faces in the nominal configuration must be respected in the realistic one.

In the realistic configuration, the two faces can be in one of the three cases described in Fig. 6 (b). In the case NCase2, the method is similar to the method defined previously: The sub-algorithm VRTFC is used. In the case NCase1, the case2 becomes the optimal case (Fig. 8). Then, the sub-algorithm

VRTFC is used after replaced the condition and the statement of the case1 by the condition and the statement of the case2.

$$\begin{cases} \text{If } \overline{N1.N2}=1, \text{ then NCase1} \\ \text{If } \overline{N1.N2}=-1, \text{ then NCase2} \end{cases} \quad (7)$$

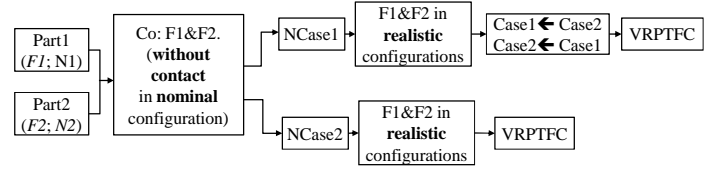


Fig. 8. The sub-algorithm VRPTFWC.

In realistic modelling, the mating constraint Co: $F&V$, Co: $F&E$ or Co: $F&F$ are to be applied in realistic model according to OFA:

Case of Co:F&V: The method is similar to the previously one (Case of Co:F&V in section 1); such as the relation (Eq. 5) is replaced by the relation (Eq. 8). In fact, Sa can be outside the face $F2$.

$$\begin{cases} d_{min} = \min \| \overline{J_{nm} P_{nm}} \| \\ Sa = J_{nm}; \text{ such as } \| \overline{J_{nm} P_{nm}} \| = d_{min} \end{cases} \quad (8)$$

- *Case of Co:F&E*: The method is similar to the previously one (Case of Co:F&E in section 1). The first vertex $V1$ is determined by the relation (Eq. 8). The second vertex $V2$ is identified by the equation (Eq. 9).

$$\begin{cases} d'_{min} = \min \| \overline{J_{nm} P_{nm}} \|; \text{ such as } J_{nm} \neq Sa \\ V2 = J_{nm}; \text{ such as } \| \overline{J_{nm} P_{nm}} \| = d'_{min} \end{cases} \quad (9)$$

According to the OFA of the parts $1'$ and $2'$, the mating constraints used are: The first mating constraint $L1$ is conserved (Co: $F'1.1&F'2.1$). The $L2$ constraint becomes a coincident condition between planar face $F'1.2$ and the edge E (Fig. 5(c)). Then, the $L3$ constraint becomes coincident condition between planar face $F'1.3$ and the vertex V (Fig. 5(c)).

B. Under constrained assembly

In the global coordinate system (X, Y, Z) of an assembly without mates, each component has six DoFs: three rotations α, β, γ and δ about X, Y and Z respectively and three translation u, v and w along X, Y and Z respectively. Then, an under constrained assembly has some of those DoF and must be respected at updating step. The method to redefining the mating constraints in the case of an under constrained assembly is shown through the case of revolute joint obtained by a coincident constraint between two planar faces and a coaxiality condition between two axes (Fig.9). The OFA composed by the two nominal parts 1 and 2 (Fig. 9) are deduced from the nominal assembly model:

- The mounting of nominal parts 1 and 2 is to be realized sequentially in the following order: $L1$ (Co: $A1&A2$) and $L2$ (Co: $F1&F2$).

- The assembly is under constrained (a rotational DOF about the Z axis is required).

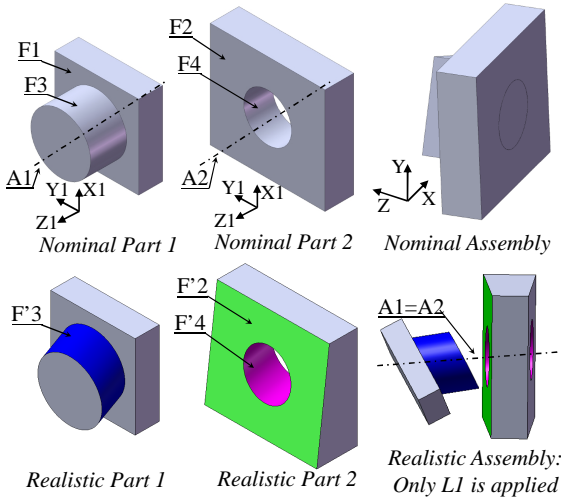


Fig. 9 Nominal and realistic models.

The faces with defects $F'1$, $F'2$ and $F'3$ are obtained by the rotation of $F1$, $F2$ and $F3$ about the $X1$, $X2$ and $X3$ axes respectively. Then, the definition of $L1$ is preserved since the OFA still be respected. However, $L2$ becomes a coincidence between the plane P and the vertex Lnm . To identify this vertex, a procedure is developed (Fig. 10 (a)): The face $F1$ is modelled by a gird of Pij vertices (method detailed previously). Pij are projected on the axis A ($A=A1=A2$) to obtain the Kij vertices (Fig. 10(b)). The vertex O is the intersection between the axis A and the face $F1$. The vertex Pnm is defined by the relation (Eq. 10).

$$\begin{cases} dij = Okij \cdot \text{sign}(OKij \cdot \vec{N}) \\ Pnm; \text{ such as } d_{nm} = \max(dij); \end{cases} \quad (10)$$

The plane P is perpendicular to A through Pnm . The vertex Lnm is the projection of Pnm on $F'2$ along the face normal N . Then, the application of $L1$ and $L2$ leads to obtain a realistic assembly with respect of the OFA defined initially.

IV. CONCLUSIONS

In this paper, a model to incorporate the dimensional and geometrical tolerances in CAD model is shown. The worst case assemblies are obtained by determining the worst case configurations of the components. In DMU, the realistic assembly requires the updating of the mating constraints. The redefinition of those assembly constraints is realised according to the OFA of the mechanism: the assembly type (fully or under constrained) and the priority order of the constraints.

The presented model is an improvement of the DMU by allowing the tolerance analysis. In addition, the tolerance impacts on the results of F.E. calculation or dynamic computation can be performed. The current research works, focuses on improving the proposed method by the realistic modelling of the complex assemblies with various constraint types existing on CAD software.

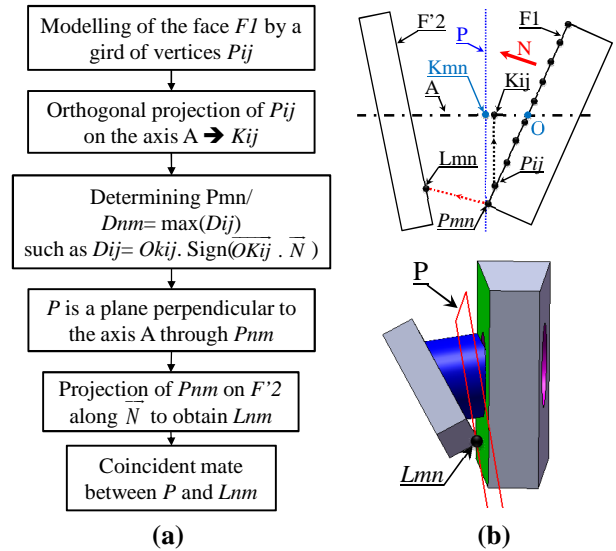


Fig. 10 Identification method of P and Lnm.

REFERENCES

- [1] B. Anselmetti, H. Louati, 'Generation of manufacturing tolerancing with ISO standards'. *International Journal of Machine Tools & Manufacture*, vol. 45, pp. 1124-1131, 2005.
- [2] F. Germain, M. Giordano, 'A new approach for three-dimensional statistical tolerancing', in *Proc. CIRP'07*, Germany, 2007.
- [3] M. Pillet, P.A. Adragna, F. Germain, 'Inertial Tolerancing: The Sorting Problem', *Journal of Machine Engineering : Manufacturing Accuracy Increasing Problems, Optimization*, Vol.6, No. 1, pp. 95-102, 2006.
- [4] M. Socoliuc, D. Buysse, A. Riviere, 'Towards a new digital functional validation process', in *Proc. CPI'07*, Morocco, 2007.
- [5] A. Clement, A. Riviere, P. Serre, 'The TTRS : a common declarative module for relative positioning, tolerancing and assembly', *International journal of CAD/CAM and computer graphics*, vol. 11, pp. 149-164, 1996.
- [6] J-Ph. Petit, S. Samper, 'Tolerancing analysis and functional requirement', in *Proc. IDMM'E'04*, 2004, paper 205.
- [7] L. Pierre, D. Teissandier, J.P. Nadeau, 'Integration of thermomechanical strains into tolerancing analysis', *International Journal on Interactive Design and Manufacturing*, Vol. 3, pp. 247-263, 2009.
- [8] A. Saka, S. Boutahari, M. Radouani, M. Carrard, 'Numerical study in VD&T manufacturing analysis for tolerance synthesis', *Revue Internationale d'Ingénierie Numérique*, Vol 2, n° 1-2, pp. 89-111, 2006.
- [9] G. Mandil, A. Desrochers, A. Rivière, 'Framework for the Monitoring of Functional Requirements Along the Product Life Cycle', in *Proc. CPI'04*, Morocco, 2004, paper 93.
- [10] B. Louhichi, M. Tlija, A. BenAmara, V. Francois, 'Reconstruction d'un modèle CAO à partir d'un maillage déformé - Application dans le cas de grands déplacements', *Mécanique & Industries*, vol. 10, p 477-486, 2009.
- [11] M. Tlija, B. Louhichi, A. Benamara, 'Integration of tolerances in the mechanical product process', in *Proc. IMPROVE'11*, 2001, pp. 499-506.
- [12] M. Tlija, B. Louhichi, A. Benamara, 'Une méthodologie de modélisation et simulation des assemblages réalistes', in *Proc. CPI'09*, 2009, paper 34.
- [13] M. Giordano, S. Samper, J.P. Petit, 'Tolerance analysis and synthesis by means of deviation domains, axi-symmetric cases', in *Proc. CIRP'05*, 2005.
- [14] J. Kim, K. Kim, K. Choi, J.Y. Lee, 'Solving 3D Geometric Constraints for Assembly Modelling', *The International Journal of Advanced Manufacturing Technology*, Volume 16, Issue 11, pp 843-849, 2000.
- [15] R. Sodhi, J-U. Turner, 'Towards modelling of assemblies for product design', *Computer-Aided Design*, vol. 26, Issue 2, pp. 85-97, 1994.